

Interaction of UV/EB-Cured Print Inks Applied to a Compostable Polymer Blend

By **Marcelo Augusto Gonçalves Bardi, Ph.D.;**
Rafael Auras, Ph.D.;
and **Luci Diva Brocardo Machado, Ph.D.**

The use of compostable polymers has increased for short lifetime product applications. Most of these products contain printed information, which are mostly produced by ultraviolet/electron beam (UV/EB)-curable printed inks. However, when compostable polymers are used, they are printed with non-biodegradable UV/EB inks, which raises the question “is the final printed structure still compostable or not?” So it is essential to understand the impact of these different coatings on the compostable polymeric substrates and their overall impact on the degradation of the whole polymer system.

The objective of this project was to assess the compostability (specifically the disintegration, mineralization and plant growth) of poly(butylene adipate-co-terephthalate) (PBAT)/thermoplastic starch (TPS) blend films coated with different UV/EB-curable

inks. This work also explores how the incorporation of a degradation-promoting additive (cobalt stearate) affects the chemical changes on the compostable polymer substrate and its effect on the overall quality of the compost used during the biodegradation process. In summary, mineralization as assessed by evolution of CO₂ of the polymer substrate was reduced up to 35% when the samples were EB-cured and/or UV-cured. EB-cured samples presented lower mineralization than the UV-cured samples, suggesting that the compostable substrate in the EB-cured samples was crosslinked by the relatively higher penetration of the ionizing radiation. The incorporation of transition-metal, salt-based pro-degrading additive caused alterations on the initiation biodegradation step (during the first 21 days) for the samples with lower curing degree.

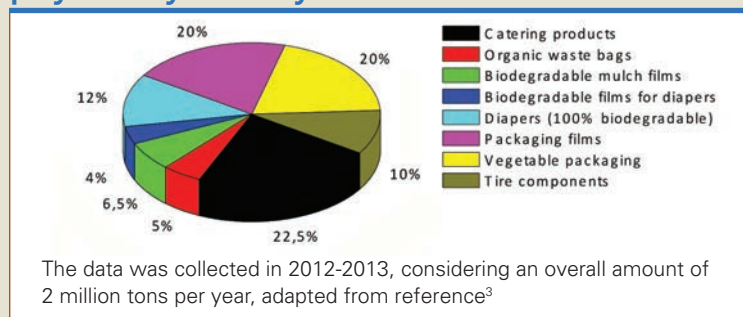
Introduction

In recent decades, UV/EB-cured products have shown exponential growth in applications traditionally dominated by solvent-based coatings such as overprinted varnish or print inks for plastic or paper packaging. This is attributed to the near zero emission of volatile organic compounds (VOCs) during the photocuring of coatings.¹

In the same context, the development of biodegradable and/or compostable polymers has increased (Figure 1). These materials

FIGURE 1

World consumption of biodegradable/compostable polymers by industry



can be classified into two groups depending on the source where they proceed—(a) from renewable sources, such as polylactide (PLA) and thermoplastic starch (TPS), and (b) from petrochemical sources, such as aromatic copolyesters and polyesteramides.

In order to be degradable, a polymer can go through abiotic and biotic degradation reaction routes (Figure 2). Specifically, to be considered compostable, a polymer has to meet a number of criteria—i.e., disintegration, biodegradation to a particular rate, ecotoxicity (heavy metals), germination and plant growth.²

When UV/EB-curable coatings are applied to biodegradable plastic substrates, there is a possibility of creating a crosslinked ink layer that could prevent the material from

biodegrading. Additionally, radiation parameters on curing can directly modify the substrate structure, causing undesirable crosslinking or premature degradation.

The use of prodegrading additives is becoming an increasingly common practice to catalyze the abiotic degradation of non-biodegradable polymers. These substances require an oxidative environment (normally by the action of ultraviolet radiation and/or heat) to reduce the weight average molecular weight (M_w) and to form oxygenated groups which could easily be metabolized by microorganisms.⁴ Equations 1 and 2 in Figure 3 present the redox mechanism induced by prodegrading additive in the polymeric bulk, where M represents the metal group in the additive structure.⁵

Thus, the aim of this project was to investigate the parameters influencing the biodegradation of a coated compostable substrate designed for short lifetime products. Poly(butylene-*co*-adipate terephthalate)/thermoplastic starch (PBAT/TPS) blend was supplied by Corn Products do Brasil (Jundiaí, SP, Brazil) and used as the polymeric substrate for printing the ink formulations as later specified. PBAT/TPS contains no more than 50% renewable polymer (starch). The detailed formulation and production technique are proprietary information. Figure 4 shows the chemical structure of both PBAT and TPS components of the polymeric blends.

Materials

The following materials were used to prepare the UV-curable clearcoating formulation—bisphenol A epoxy diacrylate resin (EBECRYL® 3720-TP25, Cytec Industries Inc.) diluted 25% by weight with tripropylene glycol diacrylate (TPGDA, Cytec Industries Inc.); trimethylolpropane triacrylate (TMPTA, Cytec Industries Inc.); blend of photoinitiators 4.5/3.5/2.0 1-hydroxycyclohexyl phenyl ketone (Irgacure 184, Ciba-Geigy Co.) / 2-hydroxy-2-methyl-1-[4-(1-methylvinyl) phenyl] propanone (Esacure KIP 150, Lamberti Co.) / 2-dimethylamino-2-(4-methylbenzyl)-1-(4-morpholin-4-yl-phenyl)-butan-1-one (Irgacure 379, Ciba Specialty Chemicals Inc.); talc (Nicon® 674, Luzenac America, Inc.); polydimethylsiloxane (Pure Silicone Fluid 100,000cSt, Clearco Products Co., Inc.); polyethylene/polytetrafluoroethylene wax (CeraSPERSE® 164, Shamrock Technology Inc.); carbon black (Printex® 45 powder, Evonik Degussa GmbH); and yellow pigment derived from diarylide m-xylylide (Irgalite® Yellow LBIW, Ciba Specialty

FIGURE 2

General pathway for polymer degradation under abiotic and biotic environments

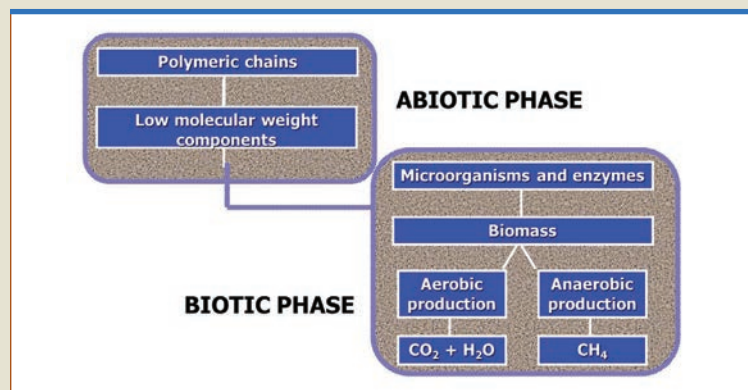


FIGURE 3

The redox mechanism induced by prodegrading additive in the polymeric bulk, where M represents the metal group in the additive structure

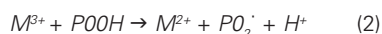
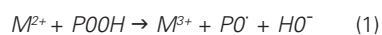
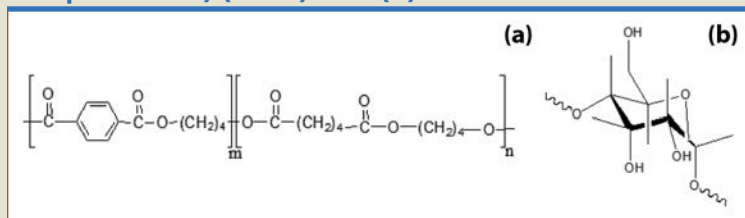


FIGURE 4

Chemical structure for (a) poly(butylene-co-adipate terephthalate) (PBAT) and (b) starch



Chemicals Inc.). The ratio of pigment to clearcoating was kept constant (21/79, wt/wt) to investigate only the influence of each pigment under UV curing. To study the effect of prodegrading additives on the inks, 1 %wt cobalt stearate (CoSt), supplied by Strem Chemicals Inc. (Newburyport, Mass., USA), was added into the ink composition described in Table 1. The inks were prepared by Flint Ink Brazil Ltda. (Cotia, SP, Brazil).

Coating Application

A manual applicator-type QuickPeek® (Boanitec Indústria e Comércio Ltda., Cotia, SP, Brazil) was used to apply the colored print inks over the PBAT/TPS films. The thickness of the coating layer was $7.0 \pm 1.3 \mu\text{m}$ before curing.

UV Curing

The coating formulations were cured at room temperature using a Labcure UV tunnel (Germetec UV and IR

Technology Ltd., Rio de Janeiro, RJ, Brazil). It was equipped with a medium-pressure mercury lamp (main photon emission range from 320 nm to 400 nm) and a conveyor belt with adjustable speed. The UV energy density was measured with an EIT UV PowerPuck® radiometer from EIT Inc. (Sterling, Va., USA). The coated plastic sheets were put on a conveyor belt able to move under the UV light beam. The irradiance of the lamp was fixed on 11.8 kW m^{-1} and the precise control of conveyor speed determined the energy density absorbed by the samples. The UV energy density of 5.20 kJ m^{-2} was applied to the samples at 23°C and 45% relative humidity (RH).

EB Curing

A Dynamitron® electron beam accelerator (Radiation Dynamics Inc., Edgewood, N.Y., USA) was used to cure the coating formulations using energy of 0.774 MeV and current of

TABLE 1

Composition of the studied coating formulations

Sample Component	UV-YE	UV-BL	EB-YE	EB-BL	UV-YE _{CoSt}	UV-BL _{CoSt}	EB-YE _{CoSt}	EB-BL _{CoSt}
	Composition (%wt)							
Epoxy acrylate resin	54	56	62	65	53	55	61	64
TMPTA monomer	10	10	10	10	10	10	10	10
Talc	3	3	3	3	3	3	3	3
Silicone	1	1	1	1	1	1	1	1
UV stabilizer	1	1	1	1	1	1	1	1
Photoinitiator blend	8	9			8	9		
PE wax	1	1	1	1	1	1	1	1
PTFE wax	1	1	1	1	1	1	1	1
Yellow pigment	21		21		21		21	
Ruby pigment		2		2		2		2
Blue pigment		3		3		3		3
Carbon black		13		13		13		13
Cobalt stearate					1	1	1	1
TOTAL	100	100	100	100	100	100	100	100

9.5 mA. After the application of the coating, the system coating with the substrate was put in a hermetically closed aluminum container filled with nitrogen as the required inert atmosphere. The containers were then put on a conveyor belt with adjustable speed and passed twice under the electron beam. The energy density was set as 12.5 kGy per pass, resulting in a total nominal energy density of 25 kGy. The energy density was 55.99 kGy s⁻¹.

UV-Accelerated Aging

The accelerated aging was performed using a QUV chamber model EQUV from Equilam Ind. e Com. Ltda. (Diadema, SP, Brazil) following ASTM D5208-09, cycle C. Fluorescent UV light bulbs with 0.89 W m⁻² nm⁻¹ irradiance (at 340 nm) were used for non-stopping 250 h cycles of irradiation under UV-incident beam at 90° and constant temperature at 50 ± 3°C. After exposition, aged and non-aged samples were characterized and evaluated.

Molecular Weight Analysis

Each sample of UV-aged PBAT/TPCS blend, control and coated, was dissolved in tetrahydrofuran (THF) at room temperature for seven days and filtered through a 0.2 µm polytetrafluoroethylene (PTFE) syringe filter. The molecular weights of the PBAT section were measured by a Waters GPC (Milford, Mass., USA) equipped with a series of three columns (HR2, HR3 and HR4), and a Waters 2414 refractive index detector interface with Waters Breeze software from Waters Inc. (Milford, Mass.), using a flow rate of 1.0 mL min⁻¹, an average run time of 45 minutes, and a temperature of 35°C. The number-average and weight-average molecular weights, \bar{M}_n and \bar{M}_w , respectively, were calculated using a calibration curve obtained from polystyrene standards (Polystyrene Shodex STD KIT SM 105,

Showa Denko, Japan) with molecular weight in the range of 1.20 to 3.64 × 10³ g mol⁻¹. A third-order polynomial calibration curve was used. The \bar{M}_n and \bar{M}_w of the PBAT part of the blends are reported.

Biodegradation

An in-house built direct measurement respirometric system (DMR) with 90 bioreactors connected to a CO₂ infrared gas analyzer was used to determine the biodegradation in organic compost. Three groups of bioreactors were used—the first containing 400 g compost (wet basis) as control sample; the second group composed of a mixture of 400 g compost (wet basis) with 8 g cellulose powder (20 µm grade, Sigma Aldrich, St. Louis, Mo., USA) as positive control; and the third one containing 400 g compost (wet basis) with 8 g of BA-PBAT/TPS, AA-PBAT/TPS, AA-Black, AA-Black-CoSt, AA-Yellow, or AA-Yellow+CoSt films cut into 1 cm x 1 cm pieces. Each sample was run in triplicate.

The biodegradation test was conducted according to ASTM D5338-11. The bioreactors were incubated in an environmental chamber at 58 ± 2°C and 55% RH for 60 days. The compost humidity was measured every three days. The CO₂ evolution was continuously monitored. The percent mineralization was calculated using the equation below where sCO_2 is the amount of CO₂ from the sample or the cellulose reactor; bCO_2 is the amount of CO₂ from the compost reactor; W is the weight of sample or cellulose; and %C is the % carbon in the film sample or cellulose obtained from elemental analyses carried out on a Perkin-Elmer 2400 CHN (Waltham, Mass., USA).

$$\%Mineralization = \frac{sCO_2 - bCO_2}{W \times \frac{\%C}{100} \times \frac{44}{12}} \times 100$$

The test complied with the ASTM D5338-11 requirements by producing 50.8 ± 4.0 mg of CO₂ per gram of volatile solids over the first 10 days of the test. The compost had an ash content of less than 70% and the pH was 7.9 ± 1.0. The total dry solids were quantified as 52.8%. The moisture content was measured by keeping 5 mg of compost in a moisture analyzer model MX50 (San Jose, Calif., USA) at 105°C until a 0.05% weight loss rate was reached, and the weight was recorded to calculate the moisture content. The dry compost was then mixed with distilled water (1:5) and left rest for 30 minutes prior to measuring the pH, using an Omega PHB212 pH meter (Stamford, Conn., USA).

Ecotoxicity

After the biodegradation test was conducted under composting conditions, the content of each replicate vessel was carefully removed and thoroughly mixed. The following tests were conducted in agreement to ASTM D6954-04 and OECD/OCDE 208 (2006). Compost (50 %wt.) containing the original samples exposed to the DMR was mixed with 50% of potting soil (Sure Mix™, Michigan Grower Products Inc., Galesburg, Mich., USA). A mixture of compost used in the DMR experiment with potting soil was used as control. One dicotyledonae and one monocotyledonae species were used for plant growth tests—*Cucumis sativus* and *Avena sativa*, respectively. Five replicates were done for each test material and control, and five seeds were used per pot. The pots were conditioned at the Michigan State University Greenhouse (Plant Science) at 25 ± 3°C during the day and 20 ± 3°C during the night. A photoperiod of 16 hours light every 8 hours darkness was adopted at a luminance of 350 ± 50 µE m⁻² s⁻¹, measured at the top of the canopy. The number of emergence,

TABLE 2

Average mineralization values for the test materials on composting environment

Material	Curing radiation	Mineralization in % after...		
		21 d	42 d	58 d
Cellulose (control)	—	49.6 ± 13.8	87.7 ± 15.8	96.4 ± 16.3
		78.5 ± 8.7	92.4 ± 17.0	91.8 ± 22.5
PBAT/TPS	—	37.2 ± 14.6	70.0 ± 28.0	104.0 ± 31.5
Black	UV	24.3 ± 6.9	49.3 ± 13.8	60.4 ± 16.3
	EB	35.5 ± 3.2	34.0 ± 6.1	35.3 ± 4.4
Black+CoSt	UV	31.4 ± 7.3	54.2 ± 15.3	65.0 ± 15.2
	EB	14.2 ± 10.4	28.1 ± 6.6	31.1 ± 5.4
Yellow	UV	28.1 ± 11.7	49.3 ± 20.2	38.4 ± 15.4
	EB	31.2 ± 3.2	22.5 ± 6.6	30.1 ± 11.2
Yellow+CoSt	UV	54.7 ± 7.7	64.5 ± 12.7	67.6 ± 6.3
	EB	45.0 ± 2.7	44.5 ± 6.4	47.5 ± 5.3

biomass (shoot dry weight and fresh weight) and shoot height of the plants as percentage of the controls were reported after 21 days of testing.

Results and Discussion

Figure 5 shows the average values and the corresponding standard deviation for CO₂ evolution from UV-aged, radiation-cured inks applied on PBAT/TPS samples. Table 2 presents the average mineralization values of the evaluated materials calculated at day 21, 42 and 58 of the biodegradation test.

Figure 5 shows that all the tested samples produced more CO₂ than the blank. This suggests that the materials are being mineralized and maybe being used as a food source by the microorganisms in the compost environment. The final mineralization for the PBAT/TPS blend surpassed the mineralization for the positive control cellulose due to a priming effect of the addition of the material.⁶ The PBAT/TPS meets the mineralization requirements as stated by ASTM D6400-12.

When a coating layer is added to the substrate, there is a reduction in the evolution of the CO₂ over the

time for all the studied compositions, independent of the pigment or the radiation curing. In some manner, the crosslinked coating reduces by half the polymer surface of the PBAT/TPS substrate film available for the action of the microorganisms.

Figure 5 also shows that the samples cured by EB radiation showed lower mineralization than the UV-cured samples. The relatively high energy density attributed to the EB radiation source may produce a highly crosslinked structure with a higher degree of curing. An increase on the crosslinking density increased the degree of protection to the film. By another side, the EB radiation penetrated deeper than the UV radiation. This higher energy is capable of reaching the PBAT/TPS substrate and caused crosslinking between the polymeric chains. So both effects are expected to reduce the mineralization of the EB-cured samples when compared to the UV-cured samples.

Furthermore, Figure 5 shows that the different scattering/absorbing properties of each pigment do not significantly interfere with the biodegradation rate. However, the

addition of a prodegrading additive increased the mineralization of compositions containing yellow pigment.⁶ This can be attributed to the interference during the curing or aging process—carbon black tends to absorb more photons and then delivers less energy to the prodegrading molecules. Cobalt stearate catalyzes the degradation chain reactions on the ink layer; by this way, chain scission in the substrate helps the posterior biodegradation steps. None of the printed samples met the mineralization requirements as specified by ASTM D6400-12.

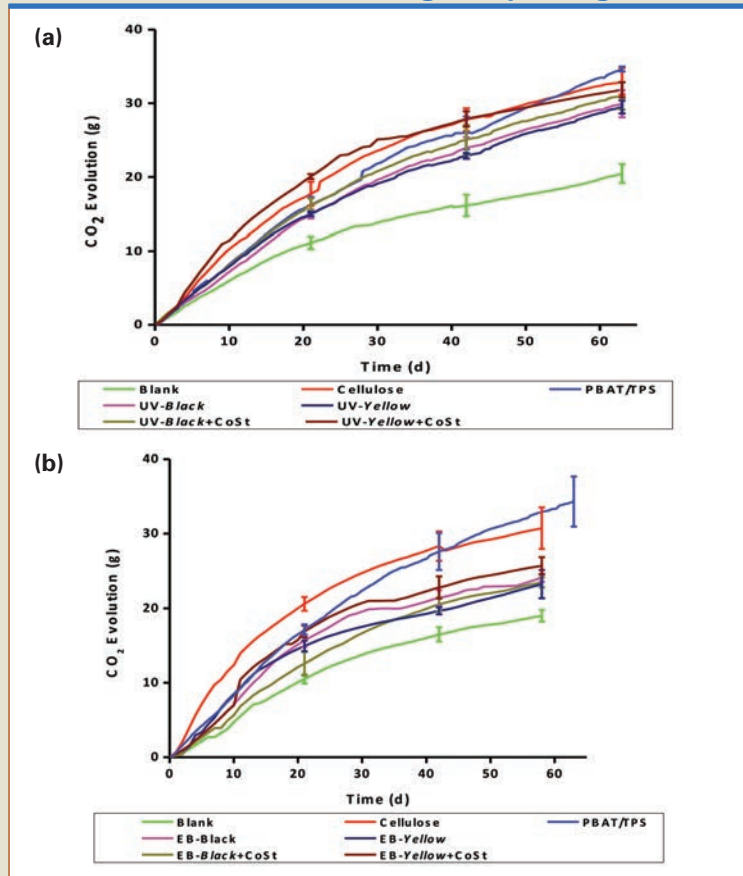
Figure 6 shows the variation in \bar{M}_n and \bar{M}_w of the PBAT part of the blends in function of the curing process, UV aging and composting. The values for the substrate PBAT/TPS are shown as comparative parameters only.

Figure 6 shows a significant reduction in the molecular weight for the uncoated substrate, reflecting the effective oxidation and biodegradation processes caused by the UV aging and biodegradation treatments.

The cured materials, either by UV- or EB-radiation, had a considerable reduction for both \bar{M}_n and \bar{M}_w of the

FIGURE 5

CO₂ evolution for (a) UV-aged, UV-cured coated samples and (b) UV-aged, EB-cured coated samples on PBAT/TPS blend film during composting test



PBAT part of the blends, as previously discussed. Both the black and the yellow pigmented inks had a similar effect on the \overline{M}_w of PBAT. However, after biodegradation, the UV-cured yellow-pigmented samples reached the lowest \overline{M}_n values when compared to the other studied samples. This result corroborates our assumptions that the interaction of radiation with the pigment particles interferes with the degree of curing and then on the crosslinking density of the coating layer, reducing the amount of radiation to reach the substrate. Further studies are needed to determine the degree of crosslinking in the ink layer and the main substrate.

Tables 3 and 4 present the results of the germination and plant growth tests of two different plant species of the compost after the biodegradation test for the control, cellulose, PBAT/TPS substrate and UV- and EB-cured coated samples.

Tables 3 and 4 indicate there is no toxic effect due to the studied samples' biodegradation on the organic compost when compared to both blank and cellulose. Interestingly, the incorporation of CoSt in the ink compositions, independently of the pigment or radiation source, increased

FIGURE 6

Average \overline{M}_n (a) and \overline{M}_w (b) of the PBAT part of the blend after UV- or EB-curing, UV aging and mineralization. Substrate PBAT/TPS is shown for comparison-basis only

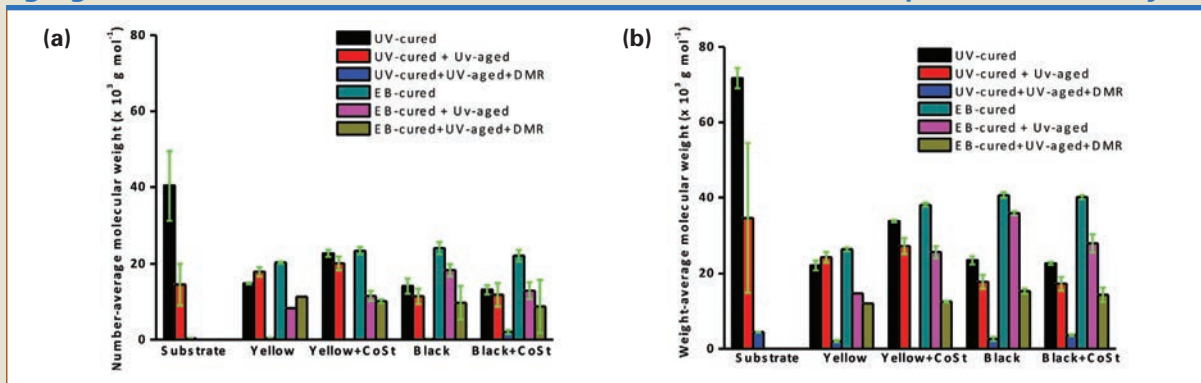


TABLE 3

Germination and plant growth tests for the control, cellulose, PBAT/TPS substrate and UV- and EB-cured coated samples using *Avena sativa* seeds

	Curing radiation	<i>Avena sativa</i>				
		Total germinated seeds (%)	Germinated seeds relative to the control (%)	Height (cm)	Wet weight (g)	Dry weight (g)
Blank (control)		75.0 ± 0.0	—	10.0 ± 1.1	0.1 ± 0.1	0.0 ± 0.0
		80.0 ± 0.0	—	23.4 ± 1.5	2.0 ± 0.2	0.3 ± 0.0
Cellulose		100.0 ± 0.0	133.3	17.3 ± 0.7	1.5 ± 0.3	0.2 ± 0.0
		90.0 ± 11.5	112.5	21.5 ± 1.1	3.7 ± 0.2	0.4 ± 0.1
PBAT/TPS		108.3 ± 14.4	144.4	6.8 ± 0.3	0.1 ± 0.0	0.1 ± 0.0
Yellow	UV	100.0 ± 0.0	133.3	18.2 ± 2.1	0.8 ± 0.1	0.1 ± 0.0
	EB	100.0 ± 0.0	125.0	21.8 ± 1.2	1.3 ± 0.2	0.2 ± 0.0
Yellow+CoSt	UV	60.0 ± 0.0	75.0	21.5 ± 1.1	2.6 ± 0.3	0.8 ± 0.1
	EB	100.0 ± 0.0	125.0	28.0 ± 1.3	2.3 ± 0.0	0.2 ± 0.0

the weight of the plants. Previous work showed that traces of cobalt can improve the quality of the plant by increasing the water uptake.⁷

Conclusion

The main criteria for disintegration and mineralization of PBAT/TPS blends were achieved as required by ASTM D6400-12 under simulated

conditions, but they were not met when a radiation-cured ink layer was applied to the blend. EB-cured samples showed lower mineralization than UV-cured ones, reflecting both the higher crosslinking density of the coating and some degree of cross-linking of the substrate. The presence of a prodegrading additive in the ink helped to catalyze the biodegradation

of those samples with lower curing degree—the yellow pigmented ones—but not sufficient to meet the standard requirements. Traces of cobalt on the ink layer seems to have increased the absorption of water and so improved the quality of the plants after the tested period. This study demonstrated that further assessment of ink layers in compostable printed polymers is

TABLE 4

Germination and plant growth tests for the control, cellulose, PBAT/TPS substrate and UV- and EB-cured coated samples using *Cucumis sativus* seeds

	Curing radiation	<i>Cucumis sativus</i>				
		Total germinated seeds (%)	Germinated seeds relative to the control (%)	Height (cm)	Wet weight (g)	Dry weight (g)
Blank (control)		100.0 ± 0.0	—	3.8 ± 0.2	2.5 ± 0.4	0.5 ± 0.1
		100.0 ± 0.0	—	6.8 ± 0.3	15.2 ± 1.4	1.3 ± 0.1
Cellulose		100.0 ± 0.0	100.0	4.2 ± 0.4	3.9 ± 0.3	0.7 ± 0.0
		100.0 ± 0.0	100.0	7.0 ± 0.2	16.4 ± 0.2	1.6 ± 0.1
PBAT/TPS		100.0 ± 0.0	100.0	4.2 ± 0.2	3.4 ± 0.2	0.6 ± 0.0
Yellow	UV	75.0 ± 0.0	75.0	4.2 ± 0.3	3.9 ± 0.4	0.7 ± 0.0
	EB	100.0 ± 0.0	100.0	6.4 ± 0.3	13.0 ± 1.0	1.1 ± 0.0
Yellow+CoSt	UV	100.0 ± 0.0	100.0	7.8 ± 0.3	12.7 ± 0.8	2.5 ± 0.2
	EB	100.0 ± 0.0	100.0	7.4 ± 0.2	16.6 ± 0.9	1.7 ± 0.1

needed since these layers can hinder polymer biodegradation.

Acknowledgments

The authors thank the Fundação de Amparo à Pesquisa do Estado de São Paulo for the financial support (Grant n. 2010/02631-0), and the Conselho Nacional de Desenvolvimento Científico e Tecnológico—CNPq for the scholarships. The authors also acknowledge Flint Ink do Brasil S.A. (Cotia, SP, Brazil) for helping in preparing the clearcoating and print inks. The authors are grateful for the collaboration of Ning Gong, Edgar Castro Aguirre, Rodolfo Lopez-Gonzalez, Rijosh John Cheruvathur and Tanatorn Tongsumrith during the direct measurement respirometry, germination test and plant growth tests; and Dave Freville for allowing the use of the greenhouse facility at MSU. ■

References

1. Adewuyi, O.S. Optimization of ultraviolet lamp placement for the curing of composites manufactured by the resin infusion between double flexible tooling (RIDFT) process. 99 (2009). at <[http://diginole.lib.fsu.edu/cgi/viewcontent.cgi?article=1402&context=etd&seiredir=1&referer=http://scholar.google.com.br/scholar?q=near+zero+emission+of+volatile+organic+compounds+%28VOC%29+during+the+photo-curing+of+coatings.&hl=pt-BR&as_sdt=0%2C5&as_ylo=2009&as_yhi=#search="near+zero+emission+volatile+organic+compounds+\(VOC\)+during+photo-curing+coatings."](http://diginole.lib.fsu.edu/cgi/viewcontent.cgi?article=1402&context=etd&seiredir=1&referer=http://scholar.google.com.br/scholar?q=near+zero+emission+of+volatile+organic+compounds+%28VOC%29+during+the+photo-curing+of+coatings.&hl=pt-BR&as_sdt=0%2C5&as_ylo=2009&as_yhi=#search=)>
2. Rudnik, E. *Compostable Polymer Materials*. 211 (Elsevier, 2008).
3. Khazir, S. and Shetty, S. Biobased polymer in the world. *Int. J. Life Sci. Biotechnol. Pharma Res.* 3, 35–43 (2014).
4. Ojeda, T. F. M. *et al.* Abiotic and biotic degradation of oxo-biodegradable polyethylenes. *Polym. Degrad. Stab.* 94, 965–970 (2009).
5. Espí, E. *et al.* Photodegradation of polyethylenes: Comparative effect of Fe and Ca-stearates as pro-oxidant additives. *Polym. Degrad. Stab.* 95, 2057–2064 (2010).
6. Bardi, M. A. G., Munhoz, M. M. L., Auras, R. A. and Machado, L. D. B. Assessment of UV exposure and aerobic biodegradation of poly(butylene adipate-co-terephthalate)/starch blend films coated with radiation-curable print inks containing degradation-promoting additives. *Ind. Crops Prod.* 60, 326–334 (2014).
7. Peralta-Videa, J. R., Lopez, M. L., Narayan, M., Saupe, G. and Gardea-Torresdey, J. The biochemistry of environmental heavy metal uptake by plants: implications for the food chain. *Int. J. Biochem. Cell Biol.* 41, 1665–77.

—*Marcelo Augusto Gonçalves Bardi, Ph.D., is a professor at Universidade São Francisco in Itatiba, Brazil; Luci Diva Brocardo Machado, Ph.D., is a chemist at the Instituto de Pesquisas Energéticas e Nucleares, in São Paulo, Brazil; and Rafael Auras, Ph.D., is an associate professor at Michigan State University, in East Lansing, Mich.*

energycuring@rahn-group.com
www.rahn-group.com

Worldwide support
for your energy curing systems

RAHN AG Zurich, Switzerland
RAHN GmbH Frankfurt am Main, Germany

RAHN USA Corp. Aurora, Illinois, USA
RAHN Trading (Shanghai) Co. Ltd. Shanghai, China

RAHN